

NNLO compatibility between pQCD theory and phenomenology in determination of the b -quark pole and $\overline{\text{MS}}$ running masses

A. Vafae^{*}

*Department of Physics, Ferdowsi University of Mashhad, P.O.Box 1436, Mashhad, Iran and
Iran's National Elites Foundation, P. O. Box 14578-93111, Tehran, Iran*

K. Javidan[†]

Department of Physics, Ferdowsi University of Mashhad, P.O.Box 1436, Mashhad, Iran

A. B. Shokouhi[‡]

Independent researcher, P. O. Box 11155-811, Tehran, Iran

(Dated: May 5, 2020)

Abstract

This contribution attempts to determine the b -quark pole mass M_b and $\overline{\text{MS}}$ running mass \overline{m}_b with two different approaches at the next-to-next-to-leading order (NNLO) corrections. At the first approach, we derive a relation between the b -quark pole mass M_b and its $\overline{\text{MS}}$ running mass \overline{m}_b at the NNLO corrections based on the perturbative Quantum Chromo Dynamics (pQCD) predictions. At the second approach, we extract numerical values of the b -quark pole and $\overline{\text{MS}}$ running masses based on the NNLO phenomenology of H1 and ZEUS Collaborations combined beauty vertex production experimental data. Then we discuss about the compatibility between the pQCD theory results and phenomenology approach in determination of the b -quark pole and $\overline{\text{MS}}$ running masses at the NNLO corrections. Also, we investigate the role and influence of the b -quark mass as an extra degree of freedom added to the input parameters of the Standard Model Lagrangian, on the improvement of the uncertainty band of the proton parton distribution functions (PDFs) and particularly on the gluon distribution.

^{*}vafae.phy@gmail.com

[†]javidan@ferdowsi.um.ac.ir

[‡]shokouhi.phy@gmail.com

I. INTRODUCTION

Measurements of the open b -quark production in deep inelastic scattering (DIS) of $e^\pm p$ at HERA provide an important test of pQCD within the framework of Standard Model and are used to constrain the proton PDFs.

Phenomenologically, the proton parton distribution functions as a non-calculable part of the factorization theorem are classically extracted by QCD fitting of a parameterized standard functional form with experimental data from deep inelastic $e^\pm p$ scattering at HERA collider [1, 2]. The experimental data extracted from DIS of $e^\pm p$ play central role in probing of the internal structure of the proton. The inclusive neutral current (NC) and charged current (CC) cross sections at HERA contain contributions from all active quark and antiquark flavors and it should be noted that up to 45 % of these contributions are originated from events with charm and beauty quarks in the final states [3, 4].

Measurements of open b -quark production in DIS of $e^\pm p$ at HERA provide an important test of pQCD theory within the Standard Model and is used to constrain the proton PDFs. On the other hand, the b -quark mass as an extra degree of freedom added to the input parameters of the Standard Model Lagrangian play central role in high energy physics phenomenology [5]. The b -quark mass as an important pQCD parameter is significantly larger than the QCD scale parameter $\Lambda_{QCD} \sim 250$ MeV and accordingly it is known as a heavy-quark which is now kinematically accessible at HERA. At the leading order (LO) or 0-loop corrections, the dominant processes for the b -quark production at HERA are generally known as the boson-gluon fusion (BGF) reactions $\gamma g \rightarrow b\bar{b}$ which are strongly sensitive to the gluon content of the proton [6].

Within the pQCD framework, the ratio of photon couplings corresponding to a heavy-quark is given by $f(h) \sim \frac{Q_h^2}{\sum Q_q^2}$ where Q_h^2 denotes the electric charge squared of a heavy-quark and Q_q^2 ($q = u, d, s, c, b$) refers to the electric charge squared of the kinematically accessible quark flavors at HERA. Accordingly for the b -quark we may write: $f(b) \sim \frac{Q_b^2}{\sum Q_q^2} = \frac{1}{9}/\frac{11}{9} = \frac{1}{11}$ or $f(b) \sim 0.09$, which clearly shows that up to 9 % of the HERA inclusive cross sections are originated from processes with the b -quark in the final states. Therefore investigation of the role and influence of the b -quark experimental data on the proton PDFs and determination of the b -quark pole mass M_b and $\overline{\text{MS}}$ running mass \overline{m}_b as an extra degree of freedom in the input parameters of the Standard Model Lagrangian play central role in many of pQCD

analysis [7].

It should be noted that in the pQCD framework the b -quark mass has been generated via a spontaneous symmetry breaking mechanism which in turn caused by a non-zero vacuum expectation value of a Higgs boson field. However, the b -quark mass remains as an extra free parameter of the the Standard Model Lagrangian and should be determined by comparing of phenomenology of experimental data with theoretical predictions of the pQCD theory. These are our main motivations to develop this article. This contribution attempts to determine the b -quark pole mass M_b and $\overline{\text{MS}}$ running mass \overline{m}_b , using phenomenology of experimental data and pQCD theory predictions at the next-to-next-to-leading order. Then we discuss for the first time about the compatibility between pQCD theory results and phenomenology approach in determination of the b -quark pole and $\overline{\text{MS}}$ running masses at the NNLO corrections. Also we investigate the role and influence of the b -quark mass as an extra pQCD parameter on the improvement of the uncertainty band of the proton PDFs and particularly on the gluon distribution.

This paper is organized as follows. In Sec. II, we describe the neutral and charged currents of deep inelastic $e^\pm p$ scattering cross sections and introduce the inclusive cross section of the b -quark production, as well. Heavy-flavor treatments to insert of heavy-quark contributions in deep inelastic electro-production proton structure functions are explained in In Sec. III. We explain and discuss about the b -quark pole and $\overline{\text{MS}}$ running masses based on the perturbative quantum chromodynamics theory predictions in Sec. IV. In Sec. V, the systematic uncertainties and our QCD analysis set-up are discussed. We present our results in Sec. VI and finally, we conclude with a summary and conclusion in Sec. VII.

II. THE INCLUSIVE CROSS SECTION OF B-QUARK PRODUCTION

The HERA particle accelerator at the Deutsches Elektronen-Synchrotron (DESY) as a large QCD laboratory, study both neutral and charged currents of $e^\pm p$ collisions and its data cover a wide range of phase space in Bjorken x scale and negative four-momentum squared of the virtual photon Q^2 [1].

The NC interactions cross sections have been published for $4.5 \cdot 10^{-4} \leq Q^2 \leq 5.0 \cdot 10^4 \text{ GeV}^2$ and $6.0 \cdot 10^{-7} \leq x \leq 6.5 \cdot 10^{-3}$ at values of the inelasticity $5.0 \cdot 10^{-3} \leq y = \frac{Q^2}{sx} \leq 9.5 \cdot 10^{-1}$. The reduced NC unpolarized deep inelastic $e^\pm p$ scattering cross sections at the centre-of-

mass energies up to $\sqrt{s} \simeq 320$ GeV after correction for Quantum Electro Dynamics (QED) radiative effects can be expressed in terms of the NC generalized structure functions \tilde{F}_2 , $x\tilde{F}_3$ and \tilde{F}_L as follows [1]:

$$\begin{aligned}\sigma_{r,NC}^{\pm} &= \frac{d^2\sigma_{NC}^{e^{\pm}p}}{dx dQ^2} \frac{Q^4 x}{2\pi\alpha^2(1+(1-y)^2)} \\ &= \tilde{F}_2 \mp \frac{(1-(1-y)^2)}{(1+(1-y)^2)} x\tilde{F}_3 - \frac{y^2}{(1+(1-y)^2)} \tilde{F}_L.\end{aligned}\quad (1)$$

Similarly the CC interactions cross sections have been published for $2.0 \cdot 10^2 \leq Q^2 \leq 5.0 \cdot 10^4$ GeV² and $1.3 \cdot 10^{-2} \leq x \leq 4.0 \cdot 10^{-1}$ at values of the inelasticity $3.7 \cdot 10^{-4} \leq y = \frac{Q^2}{sx} \leq 7.6 \cdot 10^{-3}$. The reduced cross sections for inclusive unpolarized CC $e^{\pm}p$ scattering are defined in terms of CC structure functions W_2^{\pm} , W_3^{\pm} and W_L^{\pm} as follows [1]:

$$\begin{aligned}\sigma_{r,CC}^{\pm} &= \frac{2\pi x}{G_F^2} \left[\frac{M_W^2 + Q^2}{M_W^2} \right]^2 \frac{d^2\sigma_{CC}^{e^{\pm}p}}{dx dQ^2} \\ &= \frac{(1+(1-y)^2)}{2} W_2^{\pm} \mp \frac{(1-(1-y)^2)}{2} xW_3^{\pm} - \frac{y^2}{2} W_L^{\pm}.\end{aligned}\quad (2)$$

In Eqs. (1) and (2), the quantity α refers to the fine-structure constant which is defined at zero momentum transfer frame and G_F refers to the Fermi constant which is related to the weak coupling constant g and electromagnetic coupling constant e by $G_F^2 = \frac{e^2}{4\sqrt{2}\sin^2\theta_W M_W^2} = \frac{g^2}{4M_W^2}$ [1]. More details about proton NC and CC generalized structure functions can be found in the Ref. [8].

The NC measurements of deep inelastic $e^{\pm}p$ scattering at HERA for beauty contribution to the inclusive proton cross sections $F_2^{b\bar{b}}$ have been studied by H1 and ZEUS Collaborations in the range of virtuality of the exchanged photon 2.5 GeV² $\leq Q^2 \leq 2000$ GeV² and Bjorken x scale of $3.0 \cdot 10^{-5} \leq x \leq 5.0 \cdot 10^{-2}$ [2].

In analogy to the inclusive NC and CC deep inelastic $e^{\pm}p$ scattering cross sections, the reduced cross sections for the b -quark production in deep inelastic $e^{\pm}p$ scattering measurements can be expressed in terms of the b -quark contributions to the inclusive structure functions $F_2^{b\bar{b}}$, $xF_3^{b\bar{b}}$ and $F_L^{b\bar{b}}$ as follows:

$$\begin{aligned}\sigma_{red}^{b\bar{b}} &= \frac{d\sigma^{b\bar{b}}(e^{\pm}p)}{dx dQ^2} \frac{Q^4 x}{2\pi\alpha^2(1+(1-y)^2)} \\ &= F_2^{b\bar{b}} \mp \frac{(1-(1-y)^2)}{(1+(1-y)^2)} xF_3^{b\bar{b}} - \frac{y^2}{(1+(1-y)^2)} F_L^{b\bar{b}}.\end{aligned}\quad (3)$$

Within the quark parton model (QPM) framework where $Q^2 \ll M_Z^2$ the parity-violating structure function xF_3 can be neglected and accordingly the reduced cross sections for the

b -quark contributions can be expressed by

$$\begin{aligned}\sigma_{red}^{b\bar{b}} &= \frac{d\sigma^{b\bar{b}}(e^\pm p)}{dx dQ^2} \frac{Q^4 x}{2\pi\alpha^2(1+(1-y)^2)} \\ &= F_2^{b\bar{b}} - \frac{y^2}{(1+(1-y)^2)} F_L^{b\bar{b}}.\end{aligned}\tag{4}$$

More details can be found in the Ref. [2].

The double-differential cross sections $\frac{d^2\sigma^{b\bar{b}}(e^\pm p)}{dx dQ^2}$ for the production of a b -quark may be written in terms of the b -quark contributions to the proton structure functions $F_2^{b\bar{b}}(x, Q^2)$ and $F_L^{b\bar{b}}(x, Q^2)$ as follows:

$$\frac{d^2\sigma^{b\bar{b}}(e^\pm p)}{dx dQ^2} = \frac{2\pi\alpha^2(Q^2)}{xQ^4} ([1+(1-y)^2] F_2^{b\bar{b}} - y^2 F_L^{b\bar{b}}),\tag{5}$$

where y is the lepton inelasticity. It should be noted that the superscripts $b\bar{b}$ indicate the presence of a b -quark pair in the final state. The double-differential cross sections $\frac{d^2\sigma^{b\bar{b}}(e^\pm p)}{dx dQ^2}$ is given at the Born level without electroweak radiative and QED corrections, except for the running electromagnetic coupling $\alpha(Q^2)$. More details can be found in the Ref. [2].

In this pQCD analysis, we perform three different fits entitled: PPDFs, HBPoleMass and HBRunMass so that in throughout of this article the words PPDFs, HBPoleMass and HBRunMass refer as follows:

- PPDFs: The PPDFs analysis indicates the determination of our central proton PDFs (PPDFs) based on the seven set of HERA run I and II combined data [1].
- HBPoleMass: The HBPoleMass analysis indicates the determination of the b -quark pole mass M_b using HERA I and II combined [1] and H1 and ZEUS Collaboration beauty combined production [2] data sets.
- HBRunMass: The HBRunMass analysis indicates the determination of the b -quark $\overline{\text{MS}}$ running mass \overline{m}_b using HERA I and II combined [1] and H1 and ZEUS Collaboration beauty combined production [2] data sets.

III. HEAVY-FLAVOR TREATMENTS

To insert of the heavy-quark contributions in deep inelastic electro-production proton structure functions and separating the proton structure functions into the proton PDFs and

calculable processes based on the QCD factorization theorem, there exist various heavy-flavor treatments. Within the pQCD framework there are generally two different classes of heavy-flavor treatments for deep inelastic $e^\pm p$ scattering cross sections, which are known as the so-called the fixed flavor number (FFN) and variable flavor number (VFN) schemes [9, 10].

The FONLL method was originally introduced to describe the transverse-momentum distribution of heavy-quarks in hadronic collisions and is developed based on the following formula:

$$\text{FONLL} = \text{FO} + (\text{RS} - \text{FOM0}) \times G(m, p_T), \quad (6)$$

where FO and RS stand for fixed-order and resummed approaches, respectively, FOM0 stands for a massless limit of the fixed-order calculation (an approximation of FO where only logarithmic mass terms are retained) and $G(m, p_T)$ is an arbitrary function with only this restriction that: $G(m, p_T) \rightarrow 1$ as $m/p_T \rightarrow 0$, up to terms suppressed by powers of m/p_T .

The FONLL approach contains of various variants and this NNLO QCD analysis, based on our QCD set-up and methodology which will be described in detail in Sec. V, we use FONLL-C and FONLL-C RUNM ON as two different variants of FONLL approach which have been provided by APFEL C++ code only at NNLO corrections [11] to inclusion of the b -quark contributions to the proton structure function at the NNLO QCD correction order. A very good study with more details about inclusion of heavy-quark mass contributions to deep-inelastic proton structure functions based on the FONLL method can be found in the Ref. [12].

IV. PERTURBATIVE QUANTUM CHROMODYNAMICS THEORY PREDICTIONS

One of the main features of QCD theory is color confinement postulate (the QCD short range feature) which says all hadron states and physical observables such as currents, energies, momenta and masses are color-singlet. It should be noted that the above postulate is just a kinematical constraint to eliminate colored states. There is, however a hope that the quark confinement may be the natural dynamical consequence of quantum chromodynamics theory.

Because of color confinement feature of QCD, free quarks are unobservable and accordingly there are different definitions for the b -quark mass such as pole mass and $\overline{\text{MS}}$ running mass.

Physically, the definition of the b -quark mass comes from its contribution as an extra free parameter in QCD Lagrangian as an one degree of freedom of non-Abelian gauge field theory and its exact value depends on the specific renormalization scheme.

In the on-shell renormalization scheme, the b -quark mass is defined as the pole of the b -quark propagator and known as the b -quark pole mass M_b . The b -quark pole mass definition is same as the typical definition of the lepton mass.

In the $\overline{\text{MS}}$ scheme, the b -quark mass is defined as a scale-dependent perturbative running parameter and is called the b -quark $\overline{\text{MS}}$ running mass. The b -quark $\overline{\text{MS}}$ running mass definition is the same as the definition of the running strong coupling $\alpha_s(Q^2)$.

Within the pQCD framework the connection between renormalized and unrenormalized (bare) quark mass is given by

$$m_0 = Z_m^{\overline{\text{MS}}} \overline{m}_b, \quad (7)$$

$$m_0 = Z_m^{\text{OS}} M_b, \quad (8)$$

where m_0 is the unrenormalized or bare b -quark mass and $Z_m^{\overline{\text{MS}}}$ and Z_m^{OS} are renormalization factors for the b -quark mass in the $\overline{\text{MS}}$ and the on-shell schemes, respectively.

From Eqs. (7), (8) we may write the relation between the b -quark pole mass M_b and $\overline{\text{MS}}$ running mass \overline{m}_b as follows:

$$\frac{\overline{m}_b}{M_b} = \frac{Z_m^{\text{OS}}}{Z_m^{\overline{\text{MS}}}}. \quad (9)$$

Now, it is clear from Eq. (9) to extract relation between the b -quark pole mass M_b and its $\overline{\text{MS}}$ running mass \overline{m}_b at the NNLO, it is enough to determine $Z_m^{\overline{\text{MS}}}$ and Z_m^{OS} renormalization factors in both the $\overline{\text{MS}}$ and the on-shell schemes at the NNLO.

Within the pQCD framework the mass renormalization factor $Z_m^{\overline{\text{MS}}}$ in the $\overline{\text{MS}}$ -scheme is given by:

$$Z_m^{\overline{\text{MS}}} = 1 + \sum_{i=1}^{\infty} C_i \left(\frac{\alpha_s(\mu)}{\pi} \right)^i, \quad (10)$$

with

$$\begin{aligned} C_1 &= -\frac{1}{\varepsilon}, \\ C_2 &= \frac{1}{\varepsilon^2} \left(\frac{15}{8} - \frac{1}{12} N_f \right) + \frac{1}{\varepsilon} \left(-\frac{101}{48} + \frac{5}{72} N_f \right), \end{aligned} \tag{11}$$

where N_f is the number of different fermion flavors and ε is the dimensional regularization parameter which is related to the the space-time dimension D by $\varepsilon = \frac{4-D}{2}$.

To determine the renormalization factor Z_m^{OS} in the on-shell scheme we start from the perturbative quark propagator which is defined as follows:

$$\hat{S}_F(p) = \frac{i}{\hat{p} - m_0 + \hat{\Sigma}(p, M_b)}, \tag{12}$$

where $\hat{\Sigma}(p, M_b)$ is the one particle irreducible b -quark self-energy which is parameterized as follows:

$$\hat{\Sigma}(p, M_b) = M \Sigma_1(p^2, M_b) + (\hat{p} - M_b) \Sigma_2(p^2, M_b). \tag{13}$$

Since the b -quark pole mass M_b corresponds to the position of the pole of the b -quark propagator we may write

$$Z_m^{\text{OS}} = 1 + \Sigma_1(p^2, M_b) \Big|_{p^2=M_b^2}, \tag{14}$$

which is the simplest formula for the renormalization factor Z_m^{OS} in the on-shell scheme.

Now, having computed the NNLO contribution to Z_m^{OS} and using Eqs. (9), (10), we can obtain a NNLO relation between the b -quark pole mass M_b and $\overline{\text{MS}}$ running mass \overline{m}_b in terms of the color factors as follows:

$$\begin{aligned} \overline{m}_b(M_b) &= M_b \left[1 - C_F \left(\frac{\alpha_s}{\pi} \right) + C_F \left(\frac{\alpha_s}{\pi} \right)^2 \left(C_F d_1^{(2)} \right. \right. \\ &\quad \left. \left. + C_A d_2^{(2)} + T_R N_L d_3^{(2)} + T_R N_H d_4^{(2)} \right) \right], \end{aligned} \tag{15}$$

where:

- C_F is the Casimir operator of the fundamental representation of the color gauge SU(3) group.
- C_A is the Casimir operator of the adjoint representation of the color gauge SU(3) group.

- T_R denotes the trace normalization of the fundamental representation.
- N_L refers to the number of massless quark flavors.
- N_H refers to the number of quark flavors with a pole mass equal to M_b .
- $\alpha_s \equiv \alpha_s^{(N_L+N_H)}(M_b)$ refers to the $\overline{\text{MS}}$ strong coupling which is renormalized at the scale of the pole mass $\mu = M_b$ in the pQCD theory with $N_L + N_H$ active flavors.

From Eqs. (15), we may obtain the following results for the coefficients $d_k^{(n)}$:

$$\begin{aligned}
d_1^{(2)} &= \frac{7}{128} - \frac{3}{4}\zeta_3 + \frac{1}{2}\pi^2 \log 2 - \frac{5}{16}\pi^2, \\
d_2^{(2)} &= -\frac{1111}{384} + \frac{3}{8}\zeta_3 - \frac{1}{4}\pi^2 \log 2 + \frac{1}{12}\pi^2, \\
d_3^{(2)} &= \frac{71}{96} + \frac{1}{12}\pi^2, \\
d_4^{(2)} &= \frac{143}{96} - \frac{1}{6}\pi^2.
\end{aligned}$$

Now, if we insert the standard values of the pQCD color factors: $C_F = 4/3$, $C_A = 3$, $T_R = 1/2$ and setting the number of heavy-flavors to $N_H = 1$, one may find the following result:

$$\begin{aligned}
\overline{m}_b(M_b) &= M_b \left[1 - \frac{4}{3} \left(\frac{\alpha_s}{\pi} \right) + \left(\frac{\alpha_s}{\pi} \right)^2 \left(N_L \left(\frac{71}{144} + \frac{\pi^2}{18} \right) \right. \right. \\
&\quad \left. \left. - \frac{3019}{288} + \frac{1}{6}\zeta_3 - \frac{\pi^2}{9} \log 2 - \frac{\pi^2}{3} \right) \right], \tag{16}
\end{aligned}$$

or numerically we may find:

$$\overline{m}_b(M_b) = M_b \left[1 - \frac{4}{3} \left(\frac{\alpha_s}{\pi} \right) + \left(\frac{\alpha_s}{\pi} \right)^2 (1.0414 N_L - 14.3323) \right], \tag{17}$$

or:

$$M_b = \overline{m}_b(\overline{m}_b) \left[1 + \frac{4}{3} \left(\frac{\bar{\alpha}_s}{\pi} \right) + \left(\frac{\bar{\alpha}_s}{\pi} \right)^2 (-1.0414 N_L + 13.4434) \right], \tag{18}$$

with $\bar{\alpha}_s \equiv \alpha_s(\overline{m}_b)$.

It should be noted that at the leading order (LO) or 0-loop calculation, $(\frac{\alpha_s}{\pi}) \rightarrow 0$ and accordingly the difference between the b -quark pole mass and its $\overline{\text{MS}}$ running mass vanishes.

V. QCD ANALYSIS SET-UP AND SYSTEMATIC UNCERTAINTIES

In this contribution, we made three different fits to determine the b -quark pole mass M_b and $\overline{\text{MS}}$ running mass \overline{m}_b based on the following QCD set-up:

- To choose the PDFStyle and parametrize the PDFs, we use generic HERAPDF functional form:

$$xf(x) = Ax^B(1-x)^C(1+Dx+Ex^2) \quad , \quad (19)$$

with 14 free central fit parameters and 1 extra free parameter m_b at the starting scale of the QCD evolution $Q_0^2 = 1.9 \text{ GeV}^2$ [8].

- In order to fit of experimental data on theory, we us the xFitter package as a powerful QCD open source framework [13–20].
- Evolution of the parametrized PDFs has been done based on the DGLAP collinear evolution with QCDNUM [21] and APFEL packages [11] corresponding to FONLL-C and FONLL-C RUNM ON schemes, respectively.
- We choose the lower band of the b -quark mass as $M_b = 4.192 \text{ GeV}$ and then varied in steps of 0.01.
- To include light flavor contribution, we set the renormalization and factorization scales as $\mu_r = \mu_f = Q$, while for the b -quark contribution we use the typical definition as: $\mu_r = \mu_f = \mu_b = \sqrt{Q^2 + 4m_b^2}$.
- The strangeness suppression factor and the strong coupling constant fixed to $f_s = 0.4$ and $\alpha_s^{\text{NNLO}}(M_Z^2) = 0.118$, respectively.

VI. RESULTS

In the Table (I), we show data sets used in our QCD analysis, correlated χ^2 and extracted $\frac{\chi_{Total}^2}{dof}$ corresponding to HBPoleMass and HBRunMass analysis, respectively.

According to the numerical results from Table (I), the best quality of the fit in determination of the b -quark pole mass M_b and $\overline{\text{MS}}$ running mass \overline{m}_b is $\frac{\chi_{Run}^2}{dof} = \frac{1364}{1157}$ corresponding to HBRunMass analysis. Also, according to relative improvement of χ^2 -function which is

defined by $\frac{\chi_{Pole}^2 - \chi_{Run}^2}{\chi_{Pole}^2}$, we get an improvement up to $\frac{1.187 - 1.178}{1.187} \sim 0.8\%$ in the quality of the fit for determination of the b -quark $\overline{\text{MS}}$ running mass \overline{m}_b relative to the b -quark pole mass M_b .

HERA run I + II combined and H1 and ZEUS Collaboration beauty combined data		
Experiment	HB Pole Mass	HB Run Mass
HERA I+II CC e^+p [1]	51 / 39	50 / 39
HERA I+II CC e^-p [1]	49 / 42	49 / 42
HERA I+II NC e^-p [1]	218 / 159	217 / 159
HERA I+II NC e^+p 460 [1]	215 / 204	215 / 204
HERA I+II NC e^+p 575 [1]	212 / 254	211 / 254
HERA I+II NC e^+p 820 [1]	62 / 70	62 / 70
HERA I+II NC e^+p 920 [1]	419 / 377	413 / 377
H1 and ZEUS beauty combined [2]	15 / 27	15 / 27
Correlated χ^2	133	132
$\frac{\chi_{Total}^2}{dof}$	$\frac{\chi_{Pole}^2}{dof} = \frac{1374}{1157}$	$\frac{\chi_{Run}^2}{dof} = \frac{1364}{1157}$

Table I: Data sets, correlated χ^2 and extracted $\frac{\chi_{Total}^2}{dof}$ corresponding to HB Pole Mass and HB Run Mass analysis, respectively.

In the Table (II), we present NNLO numerical values of 15 fit parameters and their uncertainties, including 14 free central PDF parameters and 1 extra m_b parameter corresponding to HB Pole Mass and HB Run Mass analysis.

According to the numerical results from Table (II) for the b -quark pole mass $M_b = 4.66 \pm 0.14$ GeV and $\overline{\text{MS}}$ running mass $\overline{m}_b = 4.40 \pm 0.10$ GeV, we obtain up to $\sim 4.0\%$ pure improvement in the uncertainty value of the b -quark $\overline{\text{MS}}$ running mass \overline{m}_b relative to the b -quark pole mass M_b .

In Sec. IV, we extracted the relation between the b -quark pole mass M_b and $\overline{\text{MS}}$ running mass \overline{m}_b at the NNLO of pQCD framework as follows:

$$\overline{m}_b(M_b) = M_b \left[1 - \frac{4}{3} \left(\frac{\alpha_s}{\pi} \right) + \left(\frac{\alpha_s}{\pi} \right)^2 (1.0414 N_L - 14.3323) \right].$$

Numerical values of fit parameters corresponding to HBPoleMass and HBRunMass analysis		
Parameter	HBPoleMass	HBRunMass
B_{uv}	0.846 ± 0.039	0.848 ± 0.039
C_{uv}	4.465 ± 0.076	4.468 ± 0.077
E_{uv}	11.4 ± 1.6	11.4 ± 1.6
B_{dv}	1.04 ± 0.10	1.04 ± 0.11
C_{dv}	4.24 ± 0.39	4.21 ± 0.40
$C_{\bar{U}}$	7.25 ± 0.97	7.22 ± 0.98
$D_{\bar{U}}$	8.5 ± 2.2	7.7 ± 2.1
$A_{\bar{D}}$	0.1651 ± 0.0092	0.1806 ± 0.0095
$B_{\bar{D}}$	-0.1810 ± 0.0068	-0.1695 ± 0.0065
$C_{\bar{D}}$	5.28 ± 0.96	5.43 ± 0.98
B_g	0.12 ± 0.12	0.12 ± 0.14
C_g	5.36 ± 0.82	5.59 ± 0.90
A'_g	2.26 ± 0.40	2.30 ± 0.44
B'_g	0.005 ± 0.058	0.020 ± 0.069
m_b	pole mass $M_b = 4.66 \pm 0.14$	$\overline{\text{MS}}$ running mass $\overline{m}_b = 4.40 \pm 0.10$

Table II: The NNLO numerical values of 15 fit parameters and their uncertainties, including 14 free central PDF parameters and 1 extra m_b parameter corresponding to HBPoleMass and HBRunMass analysis.

Now, if we insert our phenomenology results for the b -quark pole and $\overline{\text{MS}}$ running masses from Table (II) into the Eq. 20 (which comes from pQCD theory predictions) we get:

$$4.40 \sim 4.66 \left[1 - \frac{4}{3} \left(\frac{0.118}{3.141} \right) + \left(\frac{0.118}{3.141} \right)^2 (1.0414 \times 3 - 14.3323) \right], \quad (20)$$

$$4.40 \sim 4.38,$$

where according to our methodology in Sec. V, we set the strong coupling constant at M_Z^2 scale to $\alpha_s^{\text{NNLO}}(M_Z^2) = 0.118$.

If we qualify the error as: $\Delta x = |x_f - x_i|$, we see that the difference of our numerical results extracted based on the phenomenology of experimental data for the b -quark pole mass

M_b and $\overline{\text{MS}}$ running mass \overline{m}_b with the pQCD theory prediction at the NNLO corrections are less than $|4.40 - 4.38| = 0.02$. In other words, the compatibility of our numerical results with the pQCD theory predictions at the NNLO corrections and with precision of 1 part in 10^2 are up to approximately 99.98 % which show an excellent agreement between our phenomenology analysis results with pQCD theory. Furthermore, the comparison of our numerical results with the measurements from the PDG [22] world average, shows a very good agreement with the expected b -quark pole masses.

In the Fig. (1), we compare the pure impact of the b -quark pole mass M_b and $\overline{\text{MS}}$ running mass \overline{m}_b on the gluon distribution as a function of x at $Q^2 = 1.9, 5.0, 8.0$ and 10 GeV^2 .

As we expected from numerical results of Table (II), the gluon distribution is sensitive to the b -quark mass, when it is considered as an extra free parameter in pQCD framework.

The d -valence and d_v -ratio of the proton PDFs without (PPDs analysis with blue color) and with (HBPoleMass analysis with purple color) inclusion of the b -quark pole mass M_b as an extra degree of freedom added to the input parameters of the Standard Model Lagrangian is shown in the Fig. (2).

In the Fig. (3), we compare the d -valence and d_v -ratio of the proton PDFs without (PPDs analysis with blue color) and with (HBRunMass analysis with yellow color) inclusion of the b -quark $\overline{\text{MS}}$ running mass \overline{m}_b as an extra degree of freedom added to the input parameters of the Standard Model Lagrangian.

From Figs. (2) and (3), we see the dramatic impact of the b -quark pole and $\overline{\text{MS}}$ running masses at the NNLO corrections on both d -valence and d -valence ratio of the proton central PDFs, which comes from strong correlation between proton PDFs and the b -quark mass when it is considered as an extra degree of freedom added to the input parameters of the pQCD Lagrangian.

The u -valence and $u_v - d_v$ -ratio of the proton PDFs without (PPDs analysis with blue color) and with (HBPoleMass analysis with red color) inclusion of the b -quark pole mass M_b as an extra degree of freedom added to the pQCD Lagrangian is shown in the Fig. (4).

In the Fig. (5), we compare the u -valence and $u_v - d_v$ -ratio of the proton PDFs without (PPDs analysis with red color) and with (HBRunMass analysis with blue color) inclusion of the b -quark $\overline{\text{MS}}$ running mass \overline{m}_b as an extra degree of freedom added to the pQCD Lagrangian.

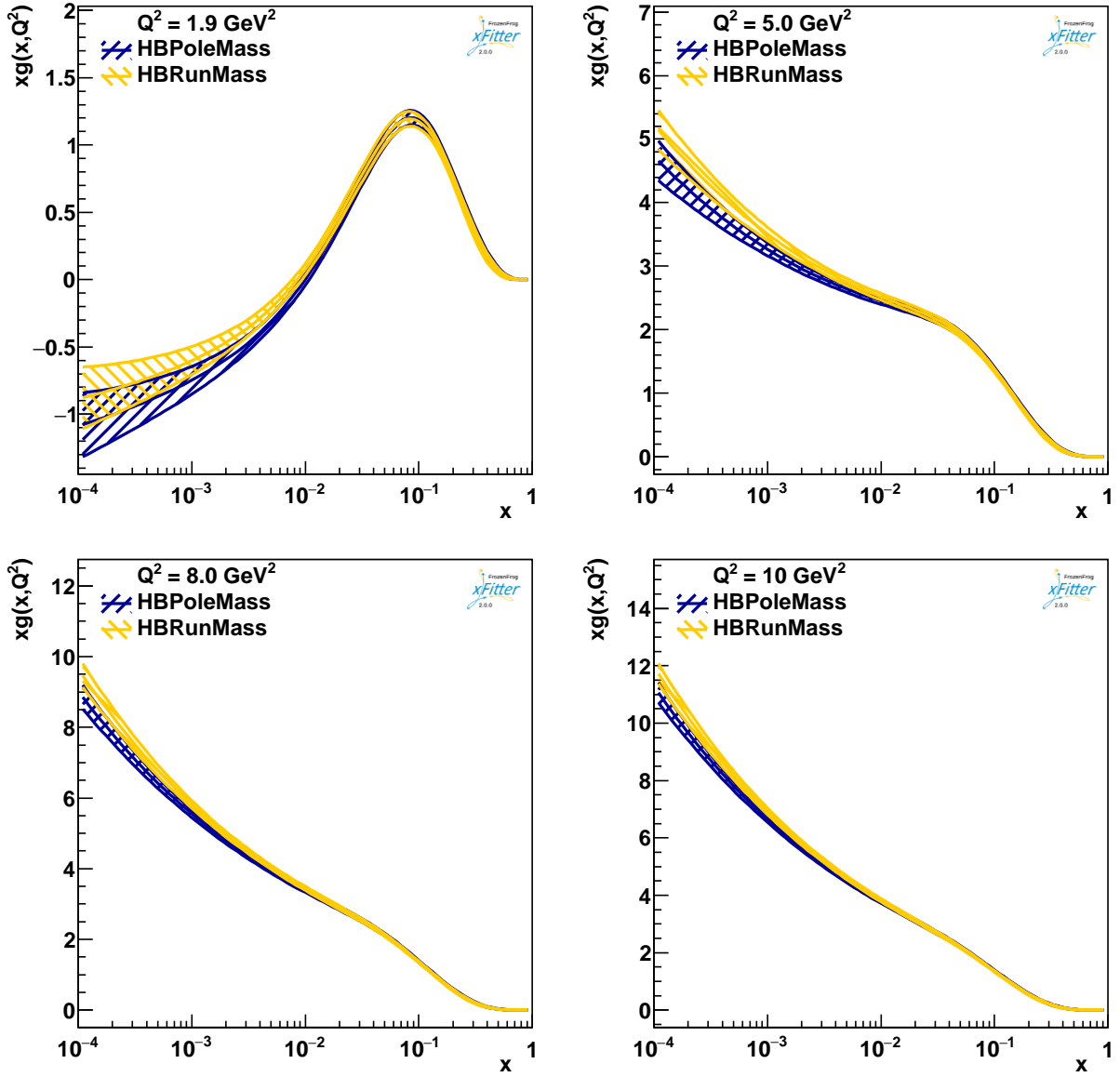


Figure 1: Comparison of pure impact of the b -quark pole mass M_b (blue color) and $\overline{\text{MS}}$ running mass \overline{m}_b (yellow color) on the gluon distribution as a function of x at $Q^2 = 1.9, 5.0, 8.0$ and 10 GeV^2 .

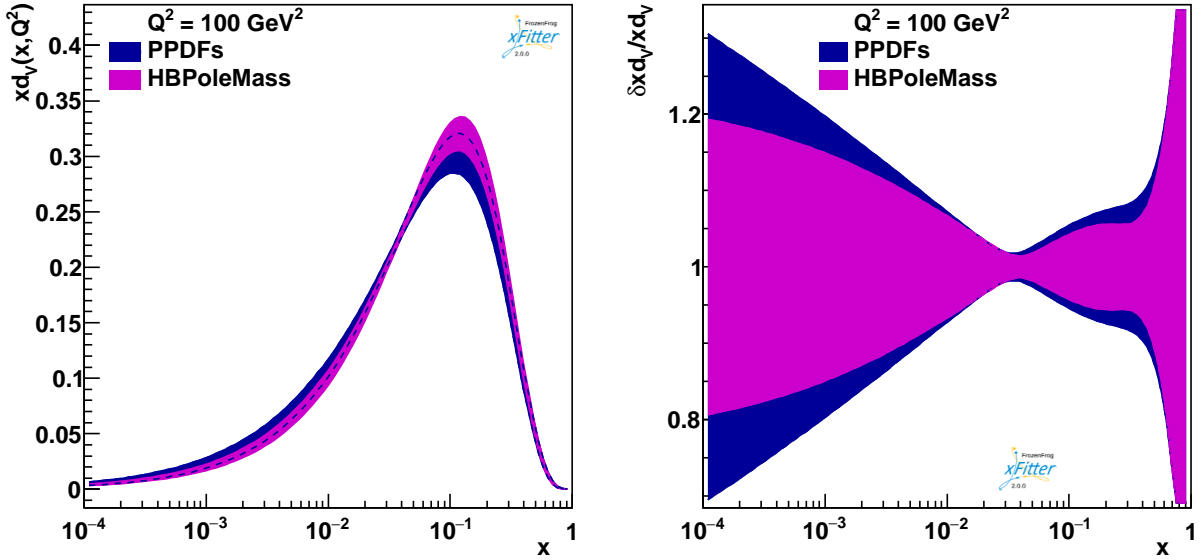


Figure 2: Comparison of the d -valence and d_v -ratio of the proton PDFs without (PPDs analysis with blue color) and with (HBPoleMass analysis with purple color) inclusion of the b -quark pole mass M_b as an extra degree of freedom added to the input parameters of the Standard Model Lagrangian.

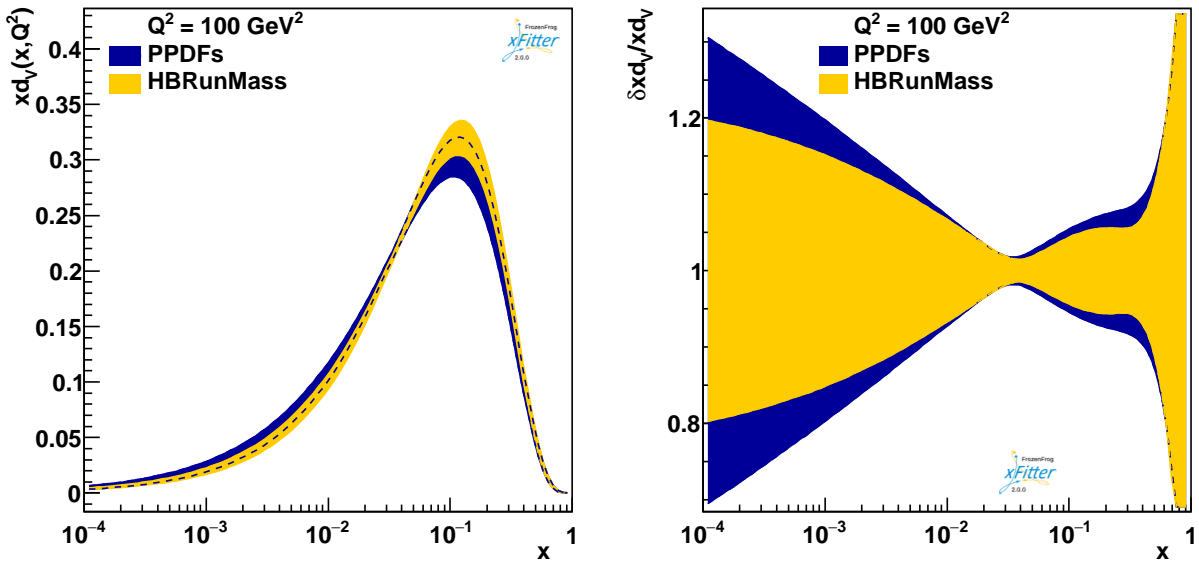


Figure 3: Comparison of the d -valence and d_v -ratio of the proton PDFs without (PPDs analysis with blue color) and with (HBRunMass analysis with yellow color) inclusion of the b -quark $\overline{\text{MS}}$ running mass \overline{m}_b as an extra degree of freedom added to the input parameters of the Standard Model Lagrangian.

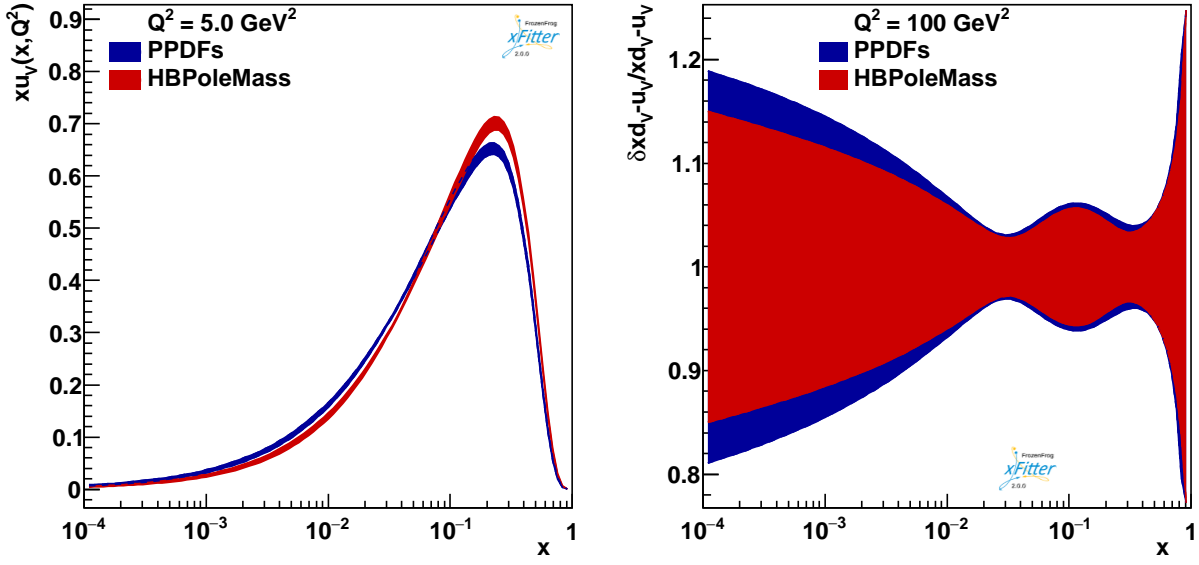


Figure 4: Comparison of the u -valence and $u_v - d_v$ -ratio of the proton PDFs without (PPDs analysis with blue color) and with (HB Pole Mass analysis with red color) inclusion of the b -quark pole mass M_b as an extra degree of freedom added to the pQCD Lagrangian.

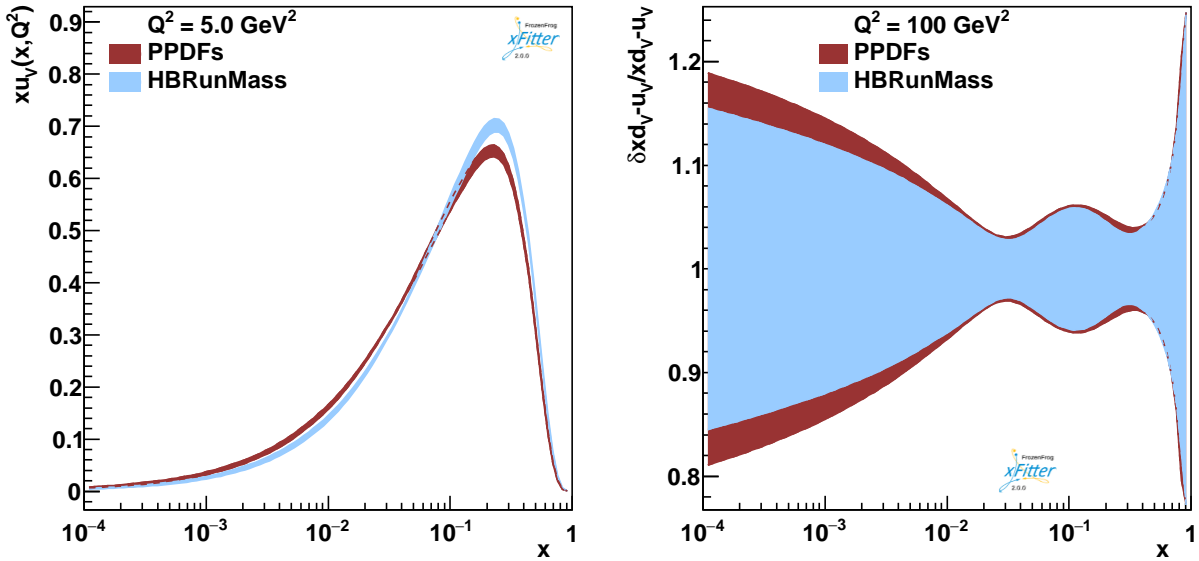


Figure 5: Comparison of the u -valence and $u_v - d_v$ -ratio of the proton PDFs without (PPDs analysis with red color) and with (HBRun Mass analysis with blue color) inclusion of the b -quark $\overline{\text{MS}}$ running mass \overline{m}_b as an extra degree of freedom added to the pQCD Lagrangian.

VII. SUMMARY AND CONCLUSION

- We determine the b -quark pole mass M_b and $\overline{\text{MS}}$ running mass \overline{m}_b with two different approaches at NNLO corrections. At the first approach, we derive a relation between the b -quark pole mass M_b and its $\overline{\text{MS}}$ running mass \overline{m}_b based on the pQCD predictions. At the second approach we extract numerical values of the b -quark pole and $\overline{\text{MS}}$ running masses based on the phenomenology of experimental data.
- Comparison of the numerical results for the b -quark pole mass M_b and its $\overline{\text{MS}}$ running mass \overline{m}_b at the NNLO corrections extracted from phenomenological base approach with pQCD theory prediction shows an excellent compatibility between these two different approaches.
- Based on the latest measurements of open b -quark production in deep inelastic scattering of $e^\pm p$ at HERA, which have been reported for the first time by H1 and ZEUS Collaborations combined beauty vertex production data, we show an excellent compatibility up to approximately 99.98 % between the pQCD theory predictions and the phenomenology approach results in determination of the b -quark pole and $\overline{\text{MS}}$ running masses at the NNLO corrections.
- Heavy-quark production measurements may be used to constrain important QCD parameters, such as the b -quark pole and $\overline{\text{MS}}$ running masses. Also such measurements has some important consequences for the determination of other pQCD parameters like the strong coupling constant $\alpha_s(M_Z^2)$. This NNLO QCD analysis reveals the role and influence of the b -quark pole and $\overline{\text{MS}}$ running masses as an extra degree of freedom added to the input parameters of the Standard Model Lagrangian in the improvement of the uncertainty band of the proton PDFs and particularly for gluon distribution and some of its ratios.

VIII. ACKNOWLEDGMENTS

We gratefully acknowledge V. Radescu for guidance and useful discussions about PDFs and xFitter. We are grateful to Prof. M. Botje from Nikhef, Science Park, Amsterdam, the Netherlands for providing the QCDNUM package as a very fast QCD evolution program. We are also grateful to Prof. F. Olness from SMU for developing invaluable heavy-flavor schemes as implemented in the xFitter package. We would like to thank Dr. Francesco Giuli, Dr. Ivan Novikov, Dr. Oleksandr Zenaiev and Dr. Sasha Glazov from xFitter developer group for guidance and technical support. We would like to appreciate Mrs. Malihe Shokouhi for spending time and careful reading the draft version of this manuscript. This work is related to the “Special Support Program for the Promotion of Scientific Authority” in Ferdowsi University of Mashhad.

-
- [1] H. Abramowicz *et al.* [H1 and ZEUS Collaborations], Eur. Phys. J. C **75**, no. 12, 580 (2015) [arXiv:1506.06042 [hep-ex]].
- [2] H. Abramowicz *et al.* [H1 and ZEUS Collaborations], Eur. Phys. J. C **78**, no. 6, 473 (2018) [arXiv:1804.01019 [hep-ex]].
- [3] M. Gluck, E. Reya and M. Stratmann, Nucl. Phys. B **422**, 37 (1994).
- [4] R. S. Thorne and R. G. Roberts, Phys. Rev. D **57**, 6871 (1998) [hep-ph/9709442].
- [5] V. N. Gribov and L. N. Lipatov, Sov. J. Nucl. Phys. **15**, 675 (1972) [Yad. Fiz. **15**, 1218 (1972)].
- [6] A. Aktas *et al.* [H1 Collaboration], Eur. Phys. J. C **47**, 597 (2006) [hep-ex/0605016].
- [7] H. Abramowicz *et al.* [ZEUS Collaboration], Eur. Phys. J. C **71**, 1573 (2011) [arXiv:1101.3692 [hep-ex]].
- [8] A. Vafae and A. N. Khorramian, Nucl. Phys. B **921**, 472 (2017) [arXiv:1709.08346 [hep-ph]].
- [9] A. D. Martin, W. J. Stirling and R. S. Thorne, Phys. Lett. B **636**, 259 (2006) [hep-ph/0603143].
- [10] M. A. G. Aivazis, F. I. Olness and W. K. Tung, Phys. Rev. D **50**, 3085 (1994) [hep-ph/9312318].
- [11] V. Bertone, S. Carrazza and J. Rojo, Comput. Phys. Commun. **185**, 1647 (2014) [arXiv:1310.1394 [hep-ph]].
- [12] S. Forte, E. Laenen, P. Nason and J. Rojo, Nucl. Phys. B **834**, 116 (2010) [arXiv:1001.2312 [hep-ph]].
- [13] xFitter, An open source QCD fit framework. <http://xFitter.org> [xFitter.org] [arXiv:1410.4412 [hep-ph]].
- [14] A. Vafae and A. B. Shokouhi, arXiv:1906.07390 [hep-ph].
- [15] A. Vafae and A. B. Shokouhi, arXiv:1904.04285 [hep-ph].
- [16] A. B. Shokouhi and A. Vafae, Nucl. Part. Phys. Proc. **300-302**, 35 (2018).
- [17] A. Vafae, Nucl. Part. Phys. Proc. **300-302**, 30 (2018).
- [18] A. Vafae, arXiv:1806.07995 [hep-ph].
- [19] A. Vafae and A. Khorramian, Nucl. Part. Phys. Proc. **282-284**, 32 (2017).
- [20] A. Vafae, A. Khorramian, S. Rostami and A. Aleedaneshvar, Nucl. Part. Phys. Proc. **270-272**, 27 (2016).
- [21] M. Botje, Comput. Phys. Commun. **182**, 490 (2011) [arXiv:1005.1481 [hep-ph]].
- [22] K. A. Olive *et al.* [Particle Data Group], Chin. Phys. C **38**, 090001 (2014).